Cell Death and Differentiation (2007) 14, 1780–1791
© 2007 Nature Publishing Group All rights reserved 1350-9047/07 $30.00
www.nature.com/cdd

Ceramide-induced G_2 arrest in rhabdomyosarcoma (RMS) cells requires $p21^{Cip1/Waf1}$ induction and is prevented by MDM2 overexpression

DC Phillips[1], JT Hunt[1], CG Moneypenny[1], KH Maclean[1], PP McKenzie[2], LC Harris[2] and JA Houghton*[,1]

The sphingoplipid ceramide is responsible for a diverse range of biochemical and cellular responses including a putative role in modulating cell cycle progression. Herein, we describe that an accumulation of ceramide, achieved through the exogenous application of C_6-ceramide or exposure to sphingomyelinase, induces a G_2 arrest in Rhabdomyosarcoma (RMS) cell lines. Utilizing the RMS cell line RD, we show that this G_2 arrest required the rapid induction of $p21^{Cip1/Waf1}$ independent of DNA damage. This was followed at later time points (48 h) by the commitment to apoptosis. Apoptosis was prevented by Bcl-2 overexpression, but permitted the maintenance of elevated $p21^{Cip1/Waf1}$ protein expression and the stabilization of the G_2 arrest response. Inhibition of $p21^{Cip1/Waf1}$ protein synthesis with cyclohexamide (CHX) or silencing of $p21^{Cip1/Waf1}$ with siRNA, prevented ceramide-mediated G_2 arrest and the late induction of apoptosis. Further, adopting the recent discovery that murine double minute 2 (MDM2) controls $p21^{Cip1/Waf1}$ expression by presenting this CDK inhibitor to the proteasome for degradation, RD cells overexpressing MDM2 abrogated ceramide-mediated $p21^{Cip1/Waf1}$ induction, G_2 arrest and the late ensuing apoptosis. Collectively, these data further support the notion that ceramide accumulation can modulate cell cycle progression. Additionally, these observations highlight MDM2 expression and proteasomal activity as key determinants of the cellular response to ceramide accumulation.
Cell Death and Differentiation (2007) **14,** 1780–1791; doi:10.1038/sj.cdd.4402198; published online 13 July 2007

The bioactive sphingolipid ceramide is a central component of the sphingomyelin cycle. In addition to playing a structural role, ceramide functions as an essential second messenger in the intracellular propagation of physiological, pharmacological and environmental signals.[1] The hydrophobic nature of ceramide limits its accumulation to membranous regions within the cell where it may influence protein distribution and function. In this regard, cytosolic concentrations of ceramide are negligible.[2] While the majority of studies evaluating the effects of an elevation in cellular ceramide have focused on its ability to induce apoptosis,[1,3] several other studies have also described ceramide to be necessary for the induction of senescence,[4] cell–cell interactions,[5] death receptor clustering[6] and autophagy.[7] Collectively these studies emphasize that the cellular response to elevations in ceramide are tissue-specific and that ceramide is capable of modulating several biochemical pathways. In this regard, data describing ceramide to mediate G_0/G_1 arrest,[3,4,8] and to accumulate following the release of cells from G_2/M arrest,[9] also implicate a role for ceramide in cell cycle progression and regulation.

Cell cycle progression is tightly controlled by cyclin-dependent kinases (CDKs), which are themselves regulated in part by two classes of CDK inhibitors (CDKI), the cip/kip family ($p21^{Cip1/Waf1}$, $p27^{Kip1}$ and $p57^{Kip2}$) and the INK family ($p16^{INK4a}$, $p15^{INKb}$, $p18^{INK4c}$ and $p19^{INK4d}$). The CDKI $p21^{Cip1/Waf1}$ can be induced through p53-dependent and -independent mechanisms and consequently mediate arrest of cycling cells primarily in G_0/G_1, but also in G_2/M.[10] Furthermore, induction of $p21^{Cip1/Waf1}$ is required to maintain the G_2 checkpoint following DNA damage.[11] Protein expression of $p21^{Cip1/Waf1}$ is regulated at transcriptional and post-translational levels. Proteasomal activity is essential in maintaining low-level basal $p21^{Cip1/Waf1}$ protein expression by regulating its degradation.[12–15]

The murine double minute 2 (MDM2) oncogene is amplified and overexpressed in numerous human cancers[16–19] including Rhabdomyosarcoma (RMS) tumors and cell lines.[20,21] MDM2 negatively regulates p53 transcriptional activity[18,22] and promotes p53 degradation by the proteasome.[23] Additionally, MDM2 can function in a p53-independent manner, interacting directly with a number of other proteins including $p21^{Cip1/Waf1}$[15], p19/14^{Arf}[24], E2F1[25] and p73.[26] Further, MDM2 overexpression suppresses $p21^{Cip1/Waf1}$-induced growth arrest of human $p53^{-/-}$ and $p53^{-/-}/Rb^{-/-}$ cells[12] by promoting its degradation by the proteasome independent of ubiquitination and also p53/Rb status.[12,15]

[1]Division of Molecular Therapeutics, Department of Oncology, St. Jude Children's Research Hospital, 332 North Lauderdale, Memphis, TN 38105, USA and [2]Department of Molecular Pharmacology, St. Jude Children's Research Hospital, 332 North Lauderdale, Memphis, TN 38105, USA
*Corresponding author. Current address: JA Houghton, Department of Cancer Biology, Lerner Research Institute, Cleveland Clinic, 9500 Euclid Avenue/NB4-59, Cleveland, OH 44195, USA. Tel: +216 445 9652; Fax: +216 444 3164; E-mail: houghtj@ccf.org
Keywords: ceramide; sphingolipids; G_2 arrest; Rhabdomyosarcoma; MDM2; $p21^{Cip1/Waf1}$
Abbreviations: ASMase, acid sphingomyelinase; ARMS, alveolar Rhabdomyosarcoma; ANOVA, analysis of variance; BrdU, 5-bromo-2′-deoxy-uridine; CDK, cyclin-dependent kinase; CDKI, cyclin-dependent kinase inhibitor; CHX, cyclohexamide; DAGK, diacylglycerol kinase; DSB, double-strand breaks; ERMS, embryonal Rhabdomyosarcoma; FB_1, fumonisin B_1; IR, ionizing radiation; MDM2, murine double minute 2; NSMase, neutral sphngomyelinase; PBS, phosphate-buffered saline; Rb, retinoblastoma; RT-PCR, reverse transcription-polymerase chain reaction; RMS, Rhabdomyosarcoma; SMase, sphingomyelinase
Received 21.11.06; revised 28.5.07; accepted 07.6.07; Edited by H Ichijo; published online 13.7.07

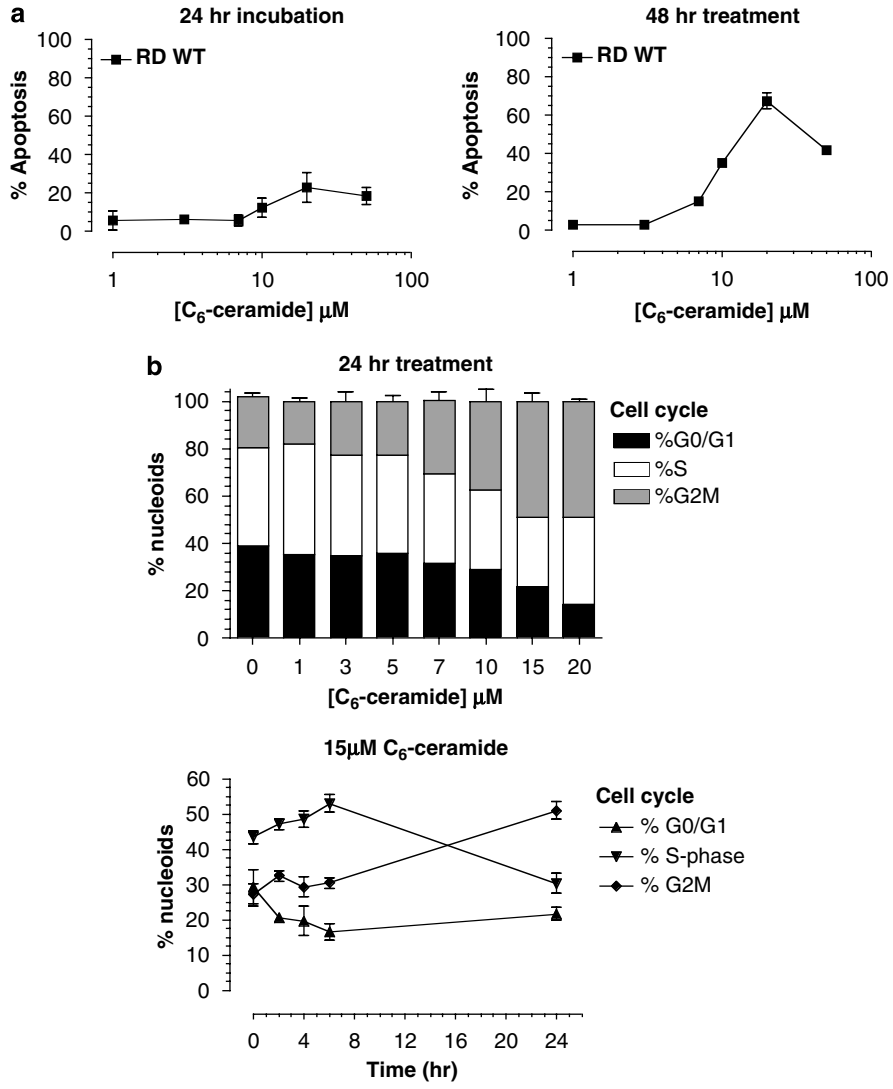

Figure 1 Ceramide induces G_2 arrest and late induction of apoptosis in the RMS cell line RD. RMS cell lines were exposed to *N*-hexanoylsphingosine (C_6-ceramide) for 0–24 h, and the percentage apoptosis and cell cycle phase were determined by DNA cell cycle analysis by flow cytometry (**a** and **b**). Additionally, RD cells were pulse-chased for 30 min with BrdU (10 μM) before wash out and treatment with C_6-ceramide (15 μM) for a further 0, 6 or 24 h. Cells were harvested and the BrdU content was determined as described in Materials and methods (**c**). Alternatively, RD cells were treated with C_6-ceramide (0–15 μM) or Nocodazole (0.5 μg/ml) for 24 h. Cells were then fixed in 70% ethanol, and probed for histone H3 phosphorylation (Ser10) as a marker of M-phase as described. Quantification of the M-phase of the cell cycle was determined by flow cytometric evaluation of the percentage population positive for histone H3 phosphorylation (**d**). Data are presented as the mean $\pm$ S.E.M. of 3–5 independent experiments. Flow cytometry histograms are representative of three independent experiments

RMS is the most common soft tissue sarcoma in pediatrics arising from cells committed to skeletal muscle lineage. RMS tumors are characterized into two histological subtypes, embryonal RMS and alveolar RMS, the latter being more refractory to treatment. Current treatment strategies encompass a multimodal approach incorporating surgery, ionizing radiation (IR) and chemotherapy.[27] Evidence suggests that ceramide generation in response to IR and chemotherapeutics[1] is at least partly required for the efficient induction of apoptosis to achieve anti-tumorigenic efficacy. However, the effect of ceramide accumulation in RMS is currently unknown.

Herein we have investigated the cellular responses of RMS cell lines to an accumulation of cellular ceramide achieved through the exogenous application of short chain, synthetic ceramide (C_6-ceramide) or through the production of endogenous ceramide mediated by cellular exposure to sphingomyelinase. We describe that an accumulation of cellular ceramide mediates a G_2 arrest response before the induction of apoptosis. This response requires the stabilization of $p21^{Cip1/Waf1}$ independent of DNA damage. Overexpression of Bcl-2 prevents ceramide-induced apoptosis, but maintains the G_2 arrest phenotype. Inhibition of $p21^{Cip1/Waf1}$ accumulation either through the abrogation of protein synthesis, silencing of $p21^{Cip1/Waf1}$ expression, or by overexpression of MDM2, prevents G_2 arrest and the late apoptosis induction. Inhibition of ceramide-induced G_2 arrest by MDM2 expression is reversed by pretreatment with the proteasome inhibitor MG132 or by siRNA targeted against MDM2. Collectively, our

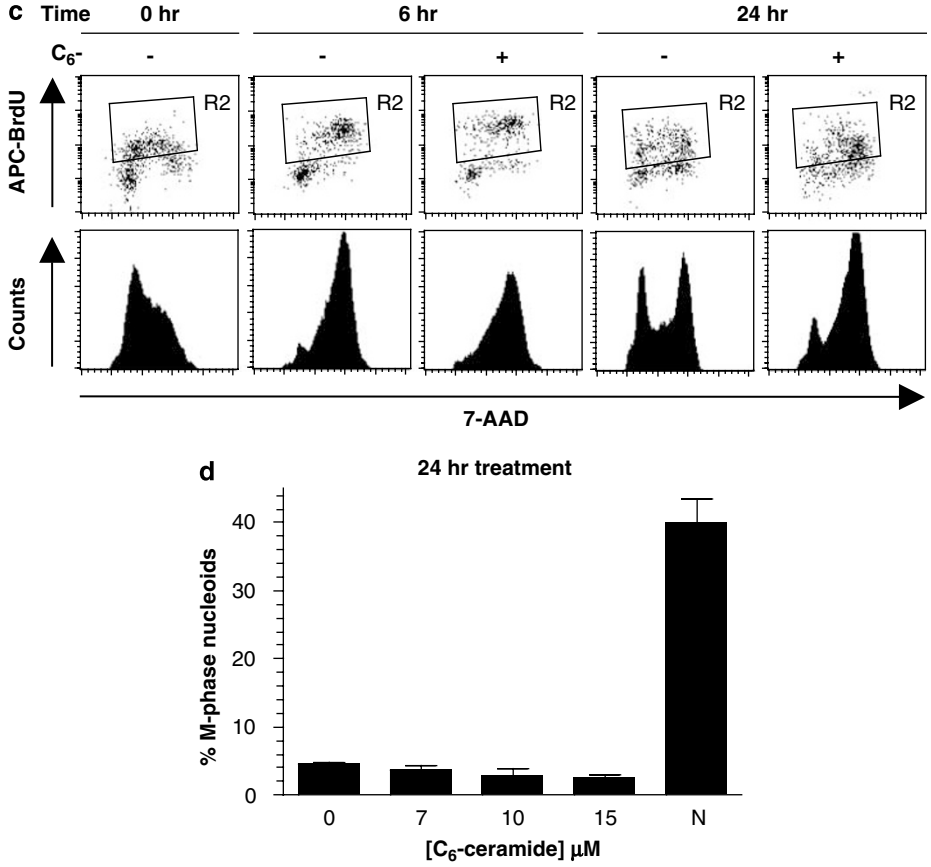

Figure 1 Continued

data describe a novel role for ceramide accumulation in mediating G_2 arrest in RMS cells that is induced by an accumulation $p21^{cip1/waf1}$ and regulated by the expression of MDM2.

Results

Treatment of the asynchronous RMS cell line RD with C_6-ceramide mediated the late induction of apoptosis after 48 h of exposure (Figure 1a). Interestingly, C_6-ceramide also induced a dose- and time-dependent elevation of cells in the G_2/M phase of the cell cycle before the appearance of apoptosis (Figure 1b). The inactive analog of C_6-ceramide, dihydro-C_6-ceramide (0–20 μM), did not modulate the cell cycle distribution or induce apoptosis (data not shown). Loss of cells in the G_0/G_1 phase of the cell cycle occurred within 2 h of C_6-ceramide (15 μM) treatment, and was accompanied by an increased number of cells in S-phase, which after 6 h also decreased as nuclei accumulated in the G_2/M phase (Figure 1b). These observations were confirmed by utilizing BrdU incorporation assays (Figure 1c). RD cells were pulse-chased with BrdU to label cells in S phase. In vehicle-treated RD cells, successful G_2/M phase exit and entry into G_0/G_1 was achieved, whereas BrdU-positive DNA remained trapped in the G_2/M phase of the cell cycle (Figure 1d). Collectively these data indicate that exit of cells from the G_2/M phase was retarded. Utilizing flow cytometric evaluation of phosphorylated-histone H3 (Ser10), an M-phase marker, we determined this arrest to be predominantly a G_2 arrest since C_6-ceramide did not increase the percentage of cells in M-phase compared to the positive control nocodazole (Figure 1d). Similar observations were observed in the RMS cell line Rh30 (data not shown).

Analysis of proteins associated with cell cycle checkpoints revealed a marked elevation in $p21^{Cip1/Waf1}$ expression levels that accompanied the dose- and time-dependent elevation in G_2-phase DNA. This was associated with a loss of cyclin-D1, although p27 remained relatively stable and the phosphorylation status of the retinoblastoma (Rb) tumor suppressor protein was not altered (Figure 2a). $p21^{Cip1/Waf1}$ mRNA levels were not modulated by C_6-ceramide treatment (data not shown). The DNA damage response pathway can induce upregulation of $p21^{Cip1/Waf1}$ levels in a p53-dependent or a p53-independent fashion.[28] However, we did not observe induction of double-strand breaks as determined by phosphorylated α-H2A.X (Ser319) staining evaluated by confocal microscopy following C_6-ceramide treatment of RD cells (Figure 2b). Further, we did not see any modulation in the expression levels of $p14^{ARF}$ ATM, p53, Chk1, Chk2 or the degree of post-translational modification (ATM-phosphorylation, p53 phosphorylation) of RD cells exposed to C_6-ceramide. Modest, and delayed phosphorylation of Chk-1

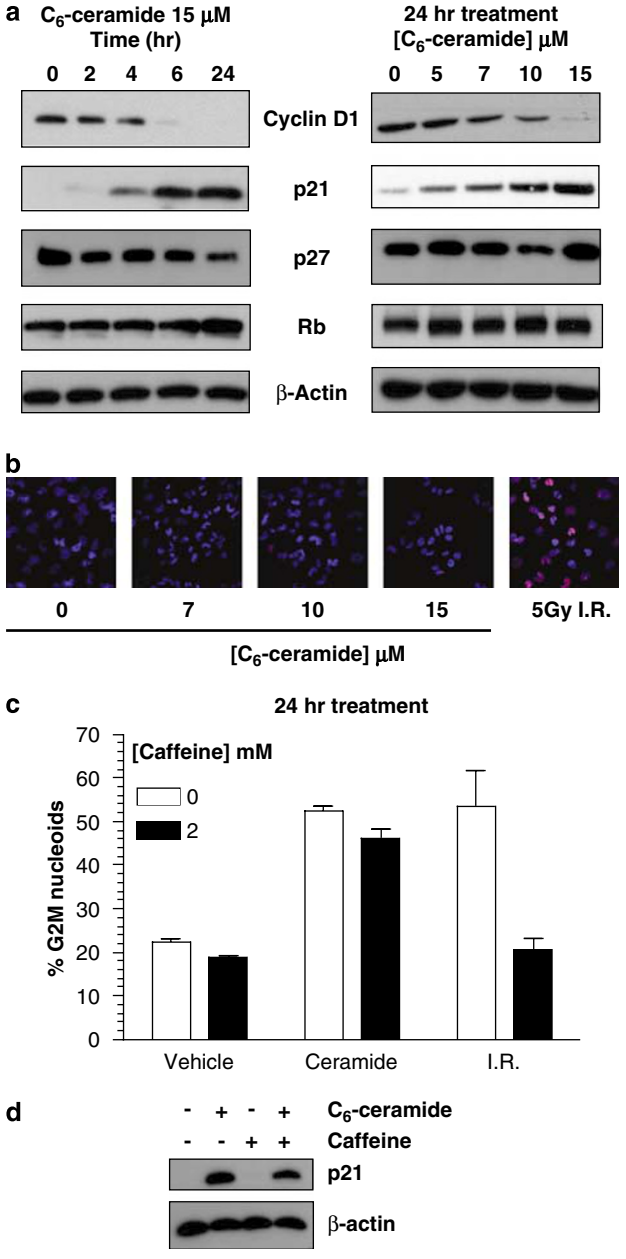

Figure 2 Ceramide-induced $p21^{Cip1/Waf1}$ accumulation independent of DNA damage. The RMS cell line RD was exposed to *N*-hexanoylsphingosine (C_6-ceramide; 0–15 μM) for 0–24 h. Cells were harvested, lysed and whole protein content was isolated before Western blot analysis for cyclin D1, $p21^{Cip1/Waf1}$, $p27^{Kip1}$, Rb or β-actin (**a**). DNA damage was determined by immunostaining for phosphorylated-histone H2A.X (Ser139; red) and was performed in RD cells treated with C_6-ceramide (0–15 μM) or 5 Gy ionizing radiation (IR), both for 24 h. Nuclei (blue) were stained with ToPro as described in Material and methods (**b**). RD cells were pretreated for 2 h with 2 mM caffeine before C_6-ceramide (15 μM) or 5 Gy IR. Cells were harvested at 24 h post-treatment, and the percentage G_2/M arrest was determined by DNA cell cycle analysis (**c**). Expression of $p21^{Cip1/Waf1}$ was evaluated by Western blot analysis (**d**). Data are presented as the mean $\pm$ S.E.M. of 3–5 independent experiments. Western blots and immunofluorescent images are representative of three independent experiments

and Chk-2, and loss of cyclin B1 expression were observed at later time points (24 h) and at high concentrations of C_6-ceramide ($\geqslant$15 μM; Supplementary Figure 1). However, these occurred after the upregulation of $p21^{Cip1/Waf1}$ (Figure 2b), which may have helped to maintain the cells in G_2. Caffeine pretreatment, which prevented the G_2/M arrest observed following IR (5 Gy), did not inhibit C_6-ceramide-induced G_2 arrest (Figure 2c) or prevent the upregulation of $p21^{Cip1/Waf1}$ levels (Figure 2d). Collectively, these data exclude C_6-ceramide-mediated G_2 arrest as a result of DNA damage.

Application of exogenous acidic SMase (ASMase; from human placenta) induced a transient elevation in endogenous ceramide (Figure 3a) as described elsewhere,[29] and was associated with a time- and dose-dependent arrest of RD cells in G_2 as determined from DNA cell cycle analysis (Figure 3a), BrdU incorporation (Figure 3b), phosphorylation of histone H3 (Figure 3c) and was associated with upregulation of p21 protein expression (Figure 3d). These observations were specific for ASMase since exogenous application of phospholipase C (PLC; from *Bacillus cereus*) or phospholipase D (PLD; from *Steptomyces* sp) did not modulate the cell cycle distribution of RD cells when used in the range 0–2 U/ml (data not shown). Together, these data confirm that the cellular response of RMS cell lines to exposure of short-chain synthetic ceramides equates to that achieved following upregulation in endogenous ceramides. Inhibition of ASMase or neutral SMase (NSMase) activity with imipramine or spiroepoxide respectively, but not ceramide synthase with fumonisin B_1 (FB_1), prevented the entry of cells into the G_2/M phase of the cell cycle (Figure 3e). These data indicate that ceramide generation from sphingomyelinases is involved in the basal regulation of cell cycle progression.

Hyperexpression of the anti-apoptotic protein Bcl-2 is associated with loss of anti-tumorigenic efficacy of chemotherapeutics.[30] Consequently, we evaluated the effect of Bcl-2 overexpression on ceramide-mediated G_2 arrest. Overexpression of Bcl-2 in RD cells inhibited the induction of apoptosis induced at later time points by C_6-ceramide at 48 h as evident by the reduction in appearance of fragmented DNA (Figure 4a) and the processing of PARP (Figure 4d). However, cells overexpressing Bcl-2 remained arrested in the G_2 phase of the cell cycle (Figure 4b). Arrest in G_2 of RD cells overexpressing Bcl-2 was confirmed by BrdU incorporation (Figure 4c). $p21^{Cip1/Waf1}$ was enhanced in both RD-GFP and RD-Bcl-2 cells similar to that observed in the parental cell line at 24 h. Further, $p21^{Cip1/Waf1}$ remained elevated in RD-Bcl-2 cells following 48 h C_6-ceramide treatment compared to the vehicle-treated RD-Bcl-2 cells and the vector control cells, whose $p21^{Cip1/Waf1}$ levels began to decline at this time point (Figure 4d). These data demonstrate that by preventing apoptosis, Bcl-2 expression permits RD cells to remain arrested in G_2 following ceramide accumulation.

Downregulation of $p21^{Cip1/Waf1}$ expression in RD cells using $p21^{Cip1/Waf1}$ specific siRNA resulted in the inhibition of C_6-ceramide-mediated G_2 arrest. RD cells transfected with $siRNA_{p21}$ resulted in a reduction of $p21^{Cip1/Waf1}$ RNA expression by approximately 60% compared with RD cells treated with $siRNA_{ctrl}$ (Figure 5a). Expression of $p21^{Cip1/Waf1}$ RNA was not affected by treatment with $siRNA_{Ctrl}$ when compared to untreated cells (Figure 5a). The levels of other cell cycle regulators ($p27^{KIP1}$ or p53) were not modulated by treatment with $siRNA_{Ctrl}$ or $siRNA_{p21}$ (data not shown). Induction of C_6-ceramide-mediated G_2 arrest and the ensuing apoptosis in

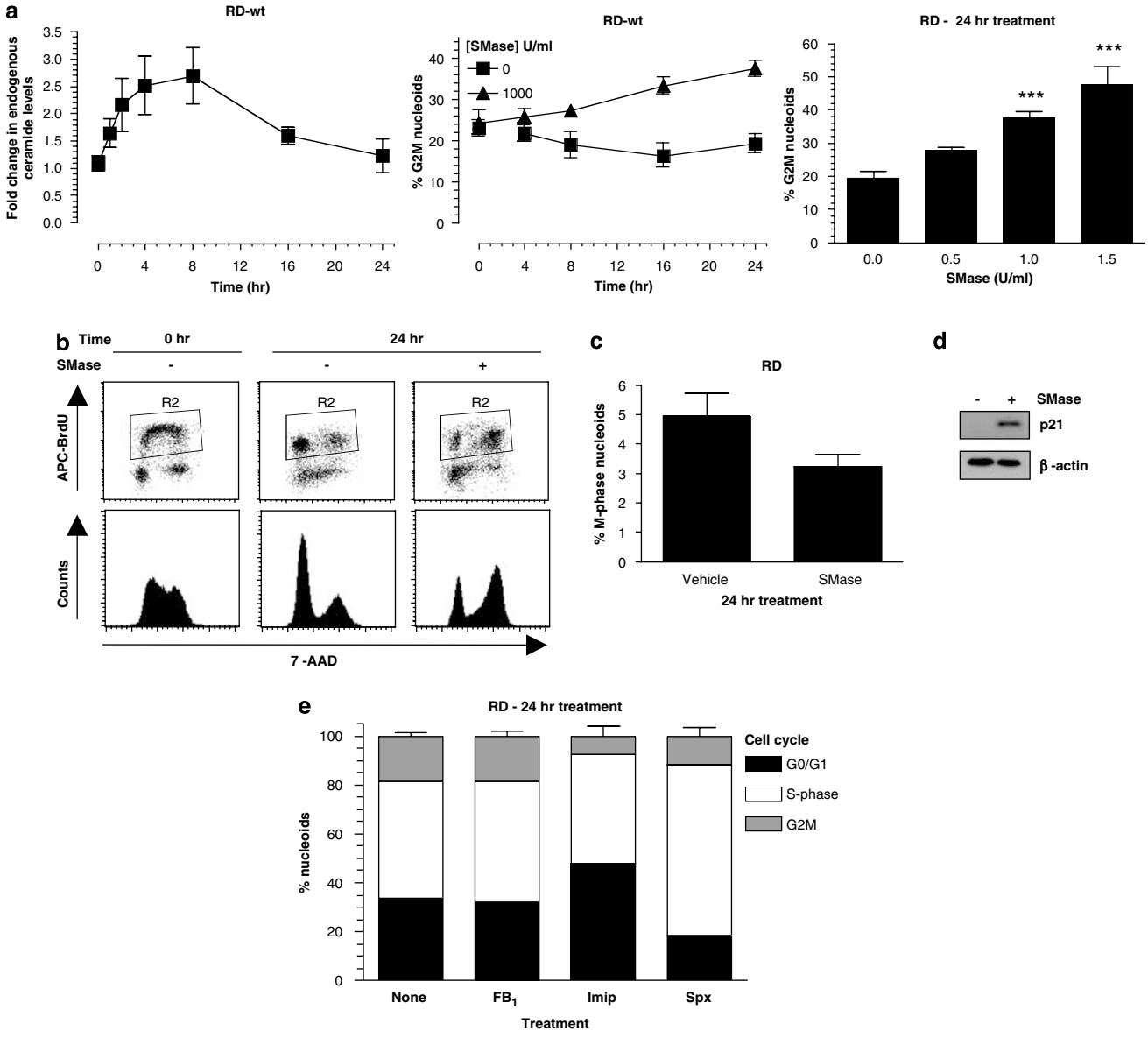

Figure 3 Acid sphingomyelinase (ASMase) induces ceramide formation, $p21^{Cip1/Waf1}$ accumulation and G_2 arrest in RD cells. The RMS cell line RD was exposed to ASMase (0–1.5 U/ml) for 0–24 h. The fold change in endogenous ceramide was determined by the DAGK assay as described in Materials and methods (**a**). The effect on the DNA cell cycle (**a**), BrdU incorporation (**b**) and M-phase (**c**) were determined as in Figure 1. In addition , cells were lysed, proteins were extracted and the expression of $p21^{Cip1/Waf1}$ was determined by Western blot analysis compared to β-actin as a loading control (**d**). The effect of the ASMase inhibitor imipramine (Imip; 25 μM), the NSMase inhibitor spiroexpoxide (Spx; 3 μM) or the ceramide synthase inhibitor FB_1 (100 μM) on the cell cycle distribution was determined (**e**). Data are presented as the mean $\pm$ S.E.M. of 3–5 independent experiments. Western blots are representative of three independent experiments

RD cells was inhibited by $siRNA_{p21}$ in RD cells when compared with $siRNA_{ctrl}$-treated cells (Figure 5b) and was accompanied by the attenuated induction of $p21^{Cip1/Waf1}$ protein expression (Figure 5c). The requirement for $p21^{Cip1/Waf1}$ in ceramide-mediated G_2 arrest and apoptosis was confirmed in HCT116 colon cancer cell lines wild type or null for $p21^{Cip1/Waf1}$. Ceramide-induced G_2-arrest and the ensuing apoptosis was inhibited in HCT116 $p21^{Cip1/Waf1}$ deficient cells when compared to the parental cell line (Figure 5d).

Expression of $p21^{Cip1/Waf1}$ is regulated at the transcriptional and post-translational level. Therefore, to evaluate the role of transcription in ceramide-induced G_2 arrest and $p21^{Cip1/Waf1}$ stabilization, RD cells were pretreated with cyclohexamide (CHX) to inhibit protein synthesis. Exposure to CHX (10 μg/ml) prevented the upregulation of $p21^{Cip1/Waf1}$ and the G_2 arrest induced by C_6-ceramide treatment (Figure 6a and b). These data demonstrate that the induction of $p21^{Cip1/Waf1}$ and the subsequent G_2 cell cycle arrest was dependent upon *de novo* protein synthesis. Turnover of $p21^{Cip1/Waf1}$ can be negatively regulated by MDM2 by promoting its proteasomal degradation.[12,15] Consequently, MDM2 was over-expressed in RD cells (Figure 7a), and the effects on

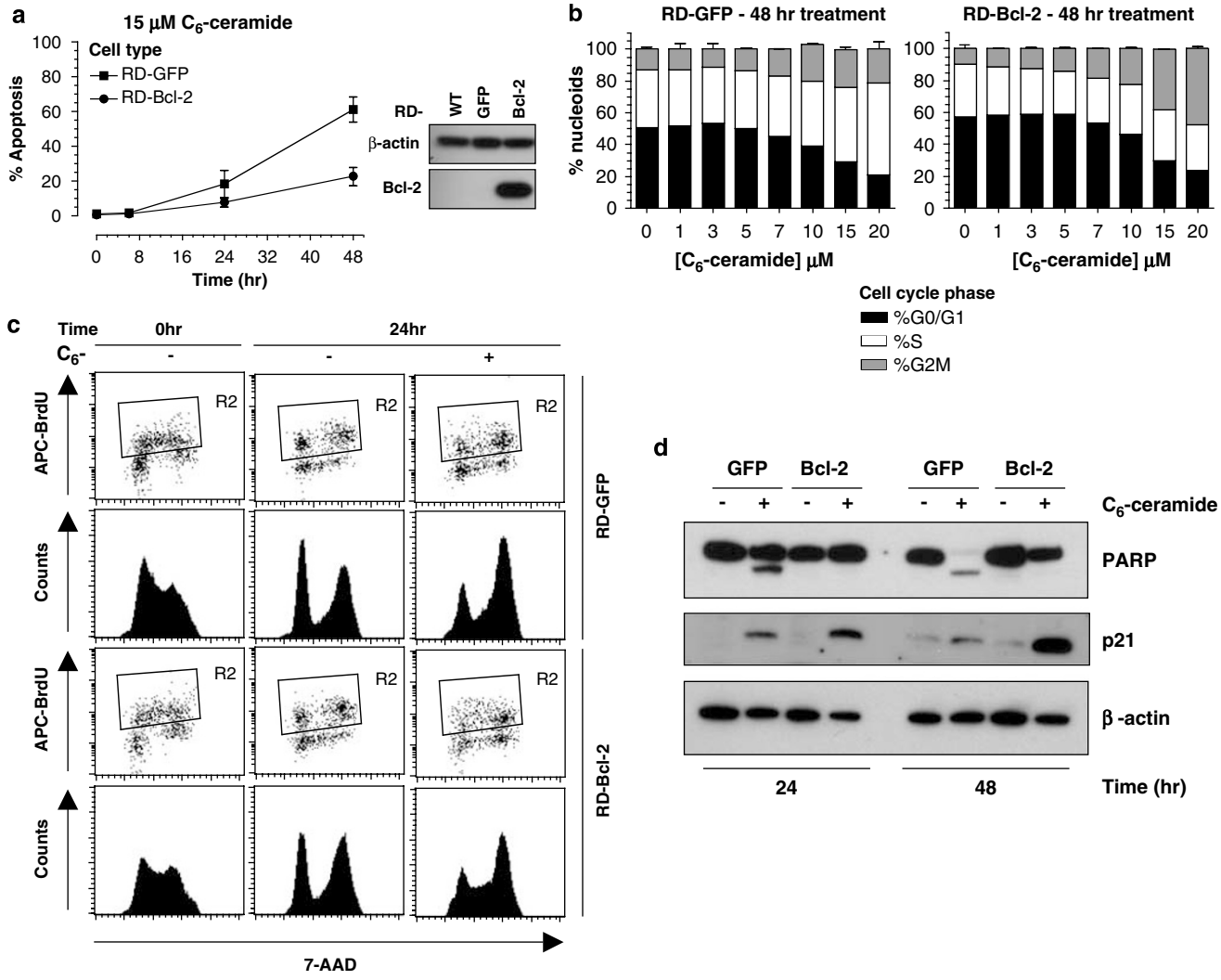

Figure 4 Bcl-2 overexpression stabilizes ceramide-mediated G_2 arrest. RD cells overexpressing GFP (RD-GFP) or Bcl-2 (RD-Bcl-2) were exposed to *N*-hexanoylsphingosine (C_6-ceramide; 0–15 μM) for 8, 24 and 48 h. Cells were harvested, and the percentage apoptosis (**a**) and cell cycle phase (**b**) were determined by DNA cell cycle analysis by flow cytometry. RD-GFP and RD-Bcl-2 cells were pulse-chased with BrdU (10 μM) as described in Figure 1(**c**). RD-GFP and RD-Bcl-2 cells were treated with C_6-ceramide (15 μM) for 24 and 48 h. Cells were harvested, lysed and protein was isolated. The expression of $p21^{Cip1/Waf1}$, PARP and β-actin was determined by Western blot analysis (**d**). Data are presented as the mean $\pm$ S.E.M. of 3–5 independent experiments. Western blots and agarose gels are representative of three independent experiments

ceramide-induced G_2 arrest by DNA cell cycle analysis and BrdU incorporation evaluated. MDM2 overexpression in RD cells significantly reduced C_6-ceramide-mediated cell cycle arrest (Figure 7a and b), prevented the C_6-ceramide-induced upregulation of $p21^{Cip1/Waf1}$ levels compared to the vector control RD cells (RD-neo; Figure 7c) and inhibited the late (48 h) induction of apoptosis (Figure 7d). Pretreatment of RD cells with the proteosome inhibitor MG132 stabilized $p21^{Cip1/Waf1}$ and promoted C_6-ceramide-/SMase-induced $p21^{Cip1/Waf1}$ protein expression and G_2/M arrest (Supplementary Figure 2). Furthermore, a low concentration of MG132 (0.1 μM) partially reversed the loss of C_6-ceramide-induced G_2/M arrest mediated by MDM2 overexpression (Figure 8a) and promoted the induction of $p21^{Cip1/Waf1}$ protein expression (Figure 8b). Higher concentrations of MG132 (0.5 μM) while not affecting the cell cycle distribution of RD cells overexpressing MDM2, induced a significant G_2/M arrest in the vector control cells. Higher concentrations of MG132 further exacerbated the extent of G_2/M arrest observed in RD-MDM2 cells mediated by C_6-ceramide (data not shown). Silencing of MDM2 using siRNA specific to MDM2 ($siRNA_{MDM2}$; Figure 8c) reversed the inhibition of G_2 arrest afforded by MDM2 overexpression in RD cells (Figure 8d). MDM2 protein levels were reduced to approximately 10% that of control treated $siRNA_{ctrl}$ RD-MDM2 cells. MDM2 protein expression was not significantly modulated by $siRNA_{ctrl}$ (Figure 8c). Silencing of MDM2 by $siRNA_{MDM2}$ potentiated the degree of G_2/M arrest mediated by C_6-ceramide thereby restoring the degree of G_2 arrest and $p21^{Cip1/Waf1}$ accumulation to that observed in the vector control and parental cell line (Figure 8d). Collectively, these data demonstrate that ceramide-mediated $p21^{Cip1/Waf1}$

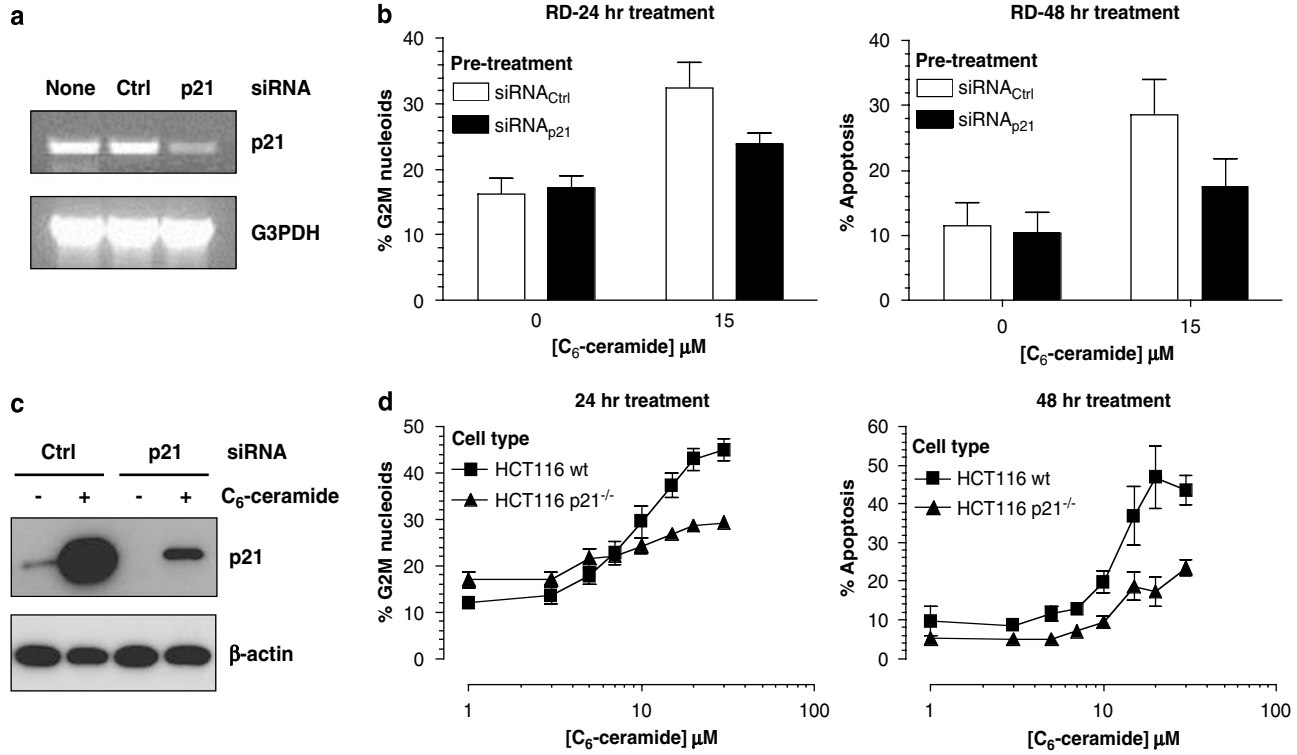

Figure 5 Silencing of $p21^{Cip1/Waf1}$ expression prevents ceramide-induced G_2-arrest. RD cells were treated with siRNA targeted against $p21^{Cip1/Waf1}$ ($siRNA_{p21}$) or scrambled siRNA ($siRNA_{ctrl}$) for 48 h and expression of $p21^{Cip1/Waf1}$ determined by RT-PCR and compared to the parental cell line utilizing G3PDH as a control (**a**). Consequently, cells were washed, media replaced, and cells were treated for a further 24 h with *N*-hexanoylsphingosine (C_6-ceramide; 15 μM). Cells were harvested, and the percentage of cells in the G_2/M phase was determined by flow cytometric DNA cell cycle analysis (**b**). Additionally, cells were lysed, proteins were isolated and subjected to Western blot analysis to detect the expression of $p21^{Cip1/Waf1}$ and β-actin (**c**). HCT116 $p21^{-/-}$ and the parental cell line HCT116 wt were treated with C_6-ceramide (0–30 μM) for 24–48 h, and the percentage apoptosis or nucleoids in the G_2/M phase of the cell cycle was determined (**d**). Data are presented as the mean $\pm$ S.E.M. of three independent experiments. Western blots are representative of two independent experiments

induction and G_2 arrest is regulated at both the transcriptional and post-translational level.

Discussion

The diverse range of cellular responses elicited by an intracellular accumulation in the sphingolipid second messenger ceramide[3–5,7,8] are underscored by tissue specificity. It has been reported that treatment strategies utilized in the treatment of RMS (IR and chemotherapy)[27] require the generation of ceramide for apoptosis to be initialized as part of their tumoricidal action.[1] However, the effects of ceramide accumulation in RMS are unresolved. The data presented here describe an essential role for the stabilization of $p21^{Cip1/Waf1}$ expression in the induction of ceramide-mediated G_2-arrest and the ensuing apoptosis in RMS cell lines. Furthermore, ceramide-induced G_2-arrest is independent of DNA damage despite the rapid induction of $p21^{Cip1/Waf1}$. MDM2 overexpression, which has been described to bind and promote $p21^{Cip1/Waf1}$ degradation by the proteasome,[12,14,15] prevented $p21^{Cip1/Waf1}$ accumulation, G_2 arrest and the ensuing late apoptosis. Prevention of $p21^{Cip1/Waf1}$ induction with CHX or $siRNA_{p21}$, or in cells deficient in $p21^{Cip1/Waf1}$ inhibited ceramide-induced G_2-arrest and the ensuing induction of apoptosis. Further, inhibition of proteasome activity with MG132 or 'knock-down' of MDM2 with siRNA reversed the inhibition of ceramide-mediated G_2-arrest afforded by MDM2 overexpression. Therefore, ceramide-mediated $p21^{Cip1/Waf1}$ stabilization and G_2 arrest are regulated at both the transcriptional and post-translational level. Utilizing RD cells overexpressing the anti-apoptotic protein Bcl-2, we demonstrate that G_2 arrest could be maintained for extended periods in the absence of apoptosis. These data indicate that apoptosis occurs either as a consequence of ceramide-mediated G_2-arrest or that these two cellular responses are independent of one another. Collectively, these data describe a novel role for ceramide in mediating cell cycle control in addition to that of apoptosis and also highlights a potential mechanism of preventing ceramide-mediated cellular responses in tissues where MDM2 is highly expressed.

The effect of ceramide on the cell cycle and $p21^{Cip1/Waf1}$ induction were immediate, occurring 2 h post-stimulation and resulting in the arrest of cells in G_2 phase, followed by the late induction of apoptosis. A preferential role for ceramide accumulation as a modulator of cell cycle progression in RMS is compounded by our observation that inhibition of basal ASMase or NSMase activity pharmacologically reduced entry of cells into the G_2/M phase of the cell cycle. Ceramide-mediated induction of $p21^{Cip1/Waf1}$ has been described by

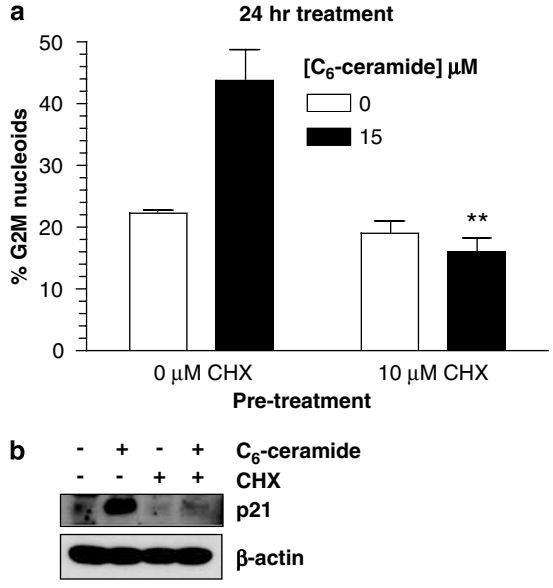

Figure 6 CHX prevents ceramide-mediated G_2 arrest and $p21^{Cip1/Waf1}$ induction. RD cells were pretreated with CHX (10 μM) for 2 h before exposure to *N*-hexanoylsphingosine (C_6-ceramide; 15 μM) for a further 24 h. Cells were harvested, and subjected to DNA cell cycle analysis (**a**) or Western blot analysis to determine the expression of $p21^{Cip1/Waf1}$ and β-actin (**b**). Data are presented as the mean $\pm$ S.E.M. of three independent experiments, where $^{**}P < 0.01$ depicts significant difference. Western blots are representative of three independent experiments

others leading to G_0/G_1 arrest in W138 fibroblasts,[4] and apoptosis in human hepatocarcinoma cells[31,32] and human Hs27 diploid fibroblasts.[33] Here we show that prevention of $p21^{Cip1/Waf1}$ accumulation through gene silencing with siRNA directed against $p21^{Cip1/Waf1}$, in cells deficient in $p21^{Cip1/Waf1}$, inhibition of protein synthesis, or enhanced proteasomal degradation by the ectopic expression of MDM2, inhibited, ceramide-induced G_2-arrest. Conversely, inhibition of proteasomal activity with MG132 enhanced ceramide-induced $p21^{Cip1/Waf1}$ accumulation and G_2 arrest. Overall, these data demonstrate a prerequisite for the stabilization of $p21^{Cip1/Waf1}$ levels for the efficient induction of ceramide-mediated G_2 arrest that requires new protein synthesis and is regulated by proteasome activity. However, complete inhibition of ceramide-induced G_2-arrest by siRNA directed against $p21^{Cip1/Waf1}$ was not achieved and may be due to an inability to completely prevent $p21^{Cip1/Waf1}$ accumulation. Additionally, it is also likely that G_2 arrest, or the transition to M-phase are controlled by numerous p53-dependent or independent mechanisms. Thus, the induction of many other genes that are associated with cell cycle progression may also contribute to the G_2 arrest phenotype observed here in RD cells following ceramide accumulation. Such candidates include GADD45 and 14–3–3σ.[34] Hyperphosphorylation of $p21^{Cip1/Waf1}$ represented by the impaired migration of $p21^{Cip1/Waf1}$ upon Western blot analysis, has been shown to be indicative of G_2/M arrest.[35] However, we did not observe this effect when using the same mouse monoclonal antibody described in the aforementioned study[35] (data not shown), or the rabbit polyclonal antibody described herein. Additional studies are required to enhance our understanding of the mechanism of ceramide-induced $p21^{Cip1/Waf1}$ accumulation and further, how $p21^{Cip1/Waf1}$ expression and the G_2 arrest phenotype are maintained.

In contrast to the majority of studies that focus upon the ability of ceramide to modulate cell cycle progression,[36,9,4,37,38] we observed a distinct lack of G_0/G_1 arrest. Ceramide-mediated dephosphorylation of Rb[36,9] is postulated to result from loss of CDK2 activity due to its inhibition by $p21^{Cip1/Waf1}$.[4] That said, in support of our observations, a partial ceramide-mediated G_2/M arrest albeit in the presence of a substantial G_0/G_1 arrest was reported in W138 human diploid fibroblasts[4] and NIH-3T3 cells.[39] The observed upregulation in $p21^{Cip1/Waf1}$ expression described here in the absence of Rb dephosphorylation or the stabilization of $p27^{Kip1}$, which has also been associated with ceramide-mediated G_0/G_1-arrest,[38] may in part account for the selective arrest of RD cells in the G_2 phase of the cell cycle rather than G_0/G_1. Collectively, these data imply that the ceramide-mediated modulation of cell cycle progression is cell type specific, and is further dictated to by the basal activity and expression of other cell cycle regulators.

Blocking damaged cells in G_2 provides time for DNA repair or the opportunity to permanently arrest cells in G_2 when damage is severe.[34] Caffeine is capable of abrogating cell cycle check points, thereby releasing cells from DNA-damaged evoked G_2-arrest.[40] Although caffeine reversed IR-induced G_2/M arrest in RD cells, it did not prevent ceramide-mediated G_2-arrest. Given the lack of phosphorylation of components of the DNA damage pathway (ATM, Chk1 and Chk2; Supplementary Figure 1) and no evidence of double-strand breaks (α-Histone H2A.X phosphorylation, Ser319), our data precludes ceramide-induced G_2-arrest and stabilization of $p21^{Cip1/Waf1}$ protein expression to be a result of DNA damage.

Overexpression of the anti-apoptotic protein Bcl-2 is associated with loss of chemotherapeutic efficacy[30] and has been described by others to prevent ceramide-induced apoptosis.[31] Similarly, we observed overexpression of Bcl-2 in RD cells to abrogate the late induction of apoptosis, but importantly, the G_2 arrest response and stabilization of $p21^{Cip1/Waf1}$ levels were sustained for extended periods following ceramide exposure. These data suggest that maintenance of G_2 arrest in the absence of apoptosis prevents mitosis and consequently attenuates oncogenic proliferation.

There are numerous reports of p53-independent regulation of p21 that can occur at both the transcriptional and post-transcriptional level.[12,31,41] Although $p21^{Cip1/Waf1}$-ubiquitin conjugates are detected in cells, and $p21^{Cip1/Waf1}$ is stabilized following proteasome inhibition, recent reports have also suggested $p21^{Cip1/Waf1}$ to be degraded via a proteasome-dependent but ubiquitin-independent mechanism.[12,14,15] MDM2 is overexpressed in a population of RMS tumors and cell lines[20,21] and has been shown to promote $p21^{Cip1/Waf1}$ degradation in a p53-independent fashion by the proteasome.[12,15] Our data extend these observations by demonstrating that MDM2 expression in RD cells inhibits ceramide-mediated G_2/M arrest, $p21^{Cip1/Waf1}$ accumulation and the ensuing late apoptosis. Further, data obtained from

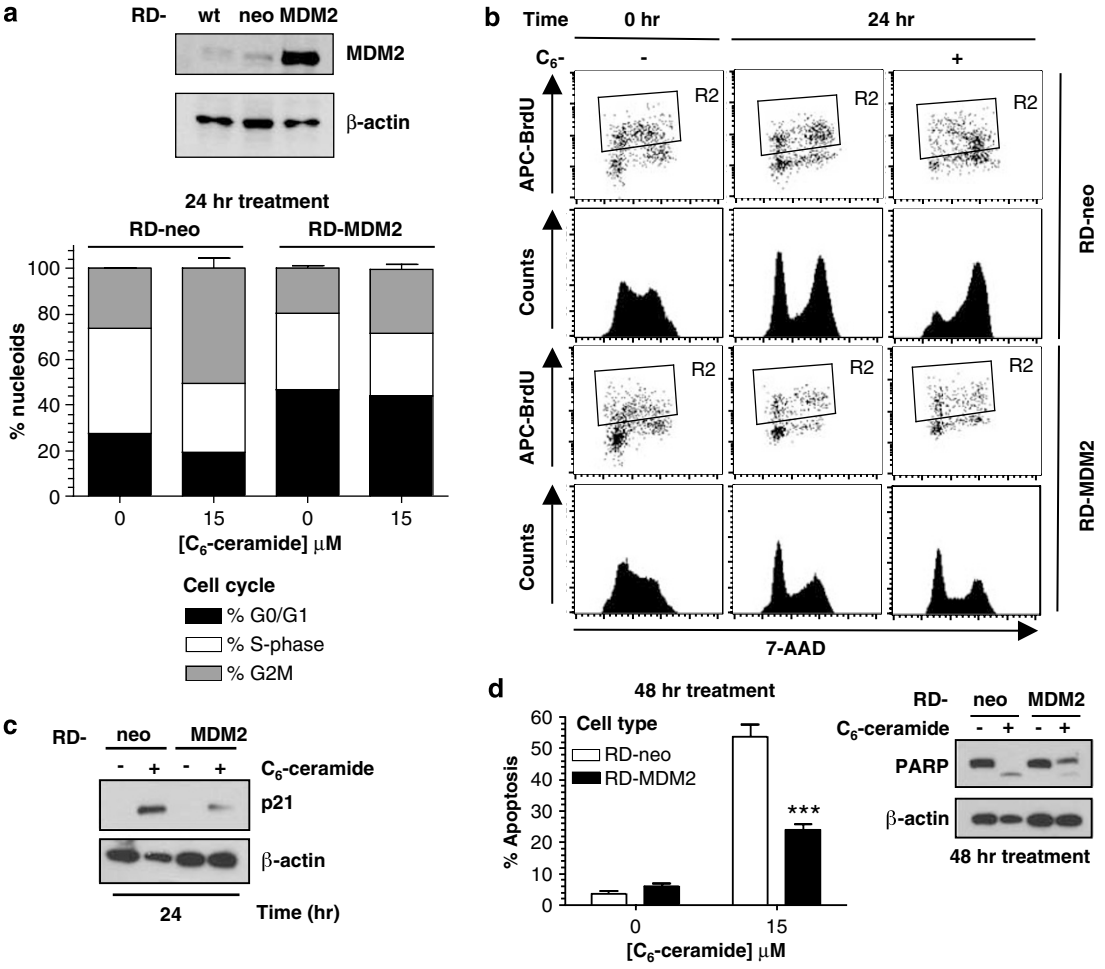

Figure 7 MDM2 overexpression prevents ceramide-induced G_2-arrest, $p21^{Cip1/Waf1}$ induction and apoptosis. RD cells overexpressing MDM2 (RD-MDM2) or the transfected vector control cells (RD-neo) were treated with *N*-hexanoylsphingosine (C_6-ceramide; 15 μM) for 24 h. MDM2 overexpression in RD-MDM2 cells was confirmed by Western blot analysis and compared to the RD-neo and parental cell line RD. β-Actin was utilized as a loading control (**a**). Following C_6-ceramide treatment, G_2 arrest was determined by DNA cell cycle analysis (**a**) and BrdU incorporation (**b**) as described in the Materials and methods. In addition, cells were lysed and the expression of $p21^{Cip1/Waf1}$ and β-actin was determined by Western blot analysis (**c**). Following ceramide treatment for 48 h, RD-neo and RD-MDM2 cells were harvested, and the percentage apoptosis was determined from the sub-G_0/G_1 content of the DNA cell cycle profiles obtained by flow cytometry, or proteins were extracted and samples were subjected to Western blot analysis to determine PARP processing using actin as a loading control (**d**). Data are presented as the mean $\pm$ S.E.M. of 3–5 independent experiments. Western blots are representative of three independent experiments

BrdU pulse–chase assays suggest that cells overexpressing MDM2 continue to cycle when compared to the vector control cells or the parental cell line. These cellular effects afforded to by MDM2 overexpression were reversed by silencing of MDM2 expression or by inhibition of proteasome activity therefore promoting $p21^{Cip1/Waf1}$ accumulation. In addition, our observation that promoting $p21^{Cip1/Waf1}$ degradation through MDM2 overexpression[12,15] in RD cells inhibits late apoptosis induction is also supportive of previous studies describing $p21^{Cip1/Waf1}$ to be required for ceramide-induced apoptosis.[31–33] Therefore, post-transcriptional repression of $p21^{Cip1/Waf1}$ by, for example, elevated levels of MDM2 or enhanced proteasomal activity, will have an oncogenic effect rather than the anticancer effect that is postulated to result from data describing $p21^{Cip1/Waf1}$ to act as an inhibitor of apoptosis.[42] Collectively, our data support the hypothesis that ceramide-mediated apoptosis occurs as a consequence of ceramide-mediated G_2 arrest. However, at this point we cannot eliminate the notion that these two cellular responses resulting from ceramide accumulation occur independently of one another.

The data presented herein further compound the pleiotropic nature of elevations in cellular ceramide in dictating a diverse series of biochemical pathways and cellular responses. We have presented data describing ceramide to induce a G_2-arrest phenotype requiring the stabilization of $p21^{Cip1/Waf1}$ protein expression independent of DNA damage. Further, we describe for the first time a role for MDM2 in abrogating ceramide-induced growth arrest and the later ensuing apoptosis. Consequently, we have identified a vital role for proteasomal activity in regulating the G_2 checkpoint and apoptotic response through the regulation of $p21^{Cip1/Waf1}$ protein levels. Collectively, by influencing the expression of the CDKI $p21^{Cip1/Waf1}$, our data support the notion that ceramide accumulation can regulate cell cycle progression in addition to apoptosis.

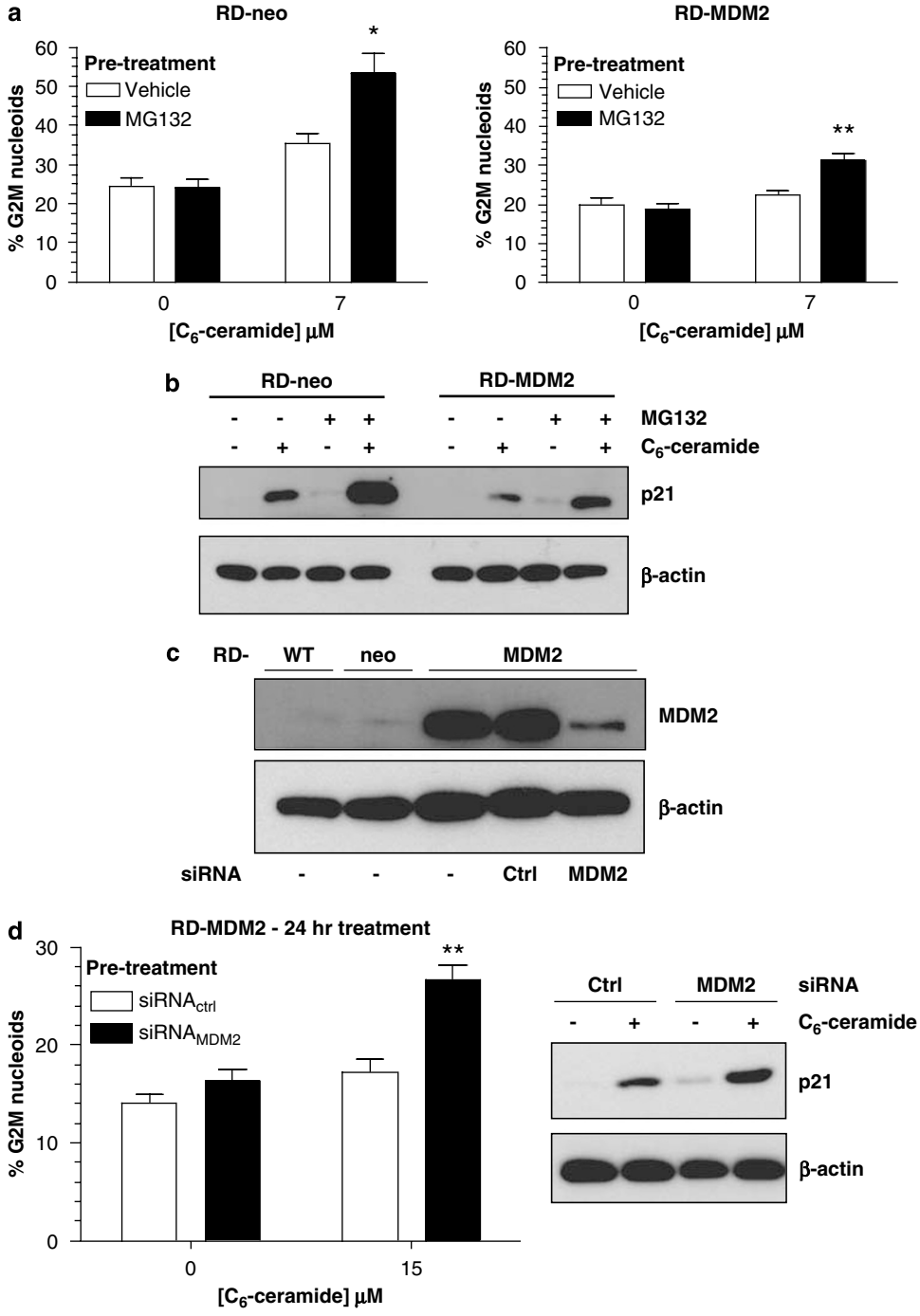

Figure 8 Proteasome inhibition or reduction of MDM2 overexpression sensitized RD-MDM2 cells to ceramide-induced G_2-arrest and $p21^{Cip1/Waf1}$ induction. RD cells overexpressing MDM2 (RD-MDM2) or the transfected vector control cells (RD-neo) were pretreated with the proteasome inhibitor MG132 (100 nM) for 2 h before the exposure to *N*-hexanoylsphingosine (C_6-ceramide; 7 μM) for a further 24 h. Cells were harvested and the effects on the G_2/M phase of the cell cycle were determined by flow cytometry (**a**) and $p21^{Cip1/Waf1}$ induction by Western blot analysis (**b**). RD-MDM2 cells were treated with siRNA directed against MDM2 ($siRNA_{MDM2}$) or scrambled siRNA ($siRNA_{Ctrl}$) for 48 h, and the expression of MDM2 was evaluated by Western blot analysis and compared to the non-treated RD-MDM2 cells, vector control cells (RD-neo) and the parental cell line RD (**c**). RD-MDM2 cells treated with siRNA were then washed, media were replaced and exposed to C_6-ceramide (15 μM) for a further 24 h. Samples were subjected to DNA cell cycle analysis and Western blot analysis to determine G_2 arrest and $p21^{Cip1/Waf1}$ induction respectively (**d**). Data are presented as the mean $\pm$ S.E.M. of three independent experiments, where $^*P<0.05$ and $^{**}P<0.01$ depict significant differences. Western blots are representative of three independent experiments utilizing β-actin as a loading control

Materials and Methods

Materials. *N*-hexanoylsphingosine (C_6-ceramide), D-erythro-*N*-hexanoyldihydrosphingosine (C_6-dihydroceramide) and FB_1 were obtained from Biomol (Plymouth meeting, PA, USA; Aurora, OH, USA). MG132, nocodazole and CHX were from EMD Biosciences (San Diego, CA, USA). Spiroexpoxide was from Axxora Life Sciences Inc. (San Diego, CA, USA). Unless stated, all other reagents were obtained from Sigma (St. Louis, MO, USA).

Cell culture and treatment. The RMS cell line RD was obtained from ATCC and Rh30 was produced by St. Jude Children's Research Hospital and has been described previously.[43] HCT116 wt and HCT116 $p21^{Cip1/Waf1-/-}$ cells were provided by Dr. Bert Vogelstein (Johns Hopkins University, Baltimore, MD, USA). Cell lines were cultured in RPMI-1640 medium containing 10% characterized FBS (Gibco/Invitrogen Corporation, Carlsbad, CA, USA) and 10 mM L-glutamine. For apoptosis assays, cells were plated at a density of 250 000 cells/well in 12-well plates, 500 000 cells/well in 6-well dishes for BrdU incorporation or M-phase analysis, and for protein extraction assays, $3 \times 10^6/10\,cm^2$ Petri dish. Ceramides were dissolved in anhydrous DMSO to a stock solution of 50 mM. Subsequent dilutions were made in 1 mM fatty acid-free BSA in PBS. After overnight attachment, cells were treated for upto 48 h with either vehicle alone, C_6-ceramide, acidic sphingomyleinase (ASMase; from human placenta; Sigma) or dihydro-C_6-ceramide. Where indicated, cells were pretreated for 120 min with MG132 (100 nM) or CHX (10 μM).

Generation of RD cells overexpressing Bcl-2 and MDM2. The retroviral expression vectors pMSCV-I-GFP (expressing GFP), pMSCV-I-Bcl-2 (expressing GFP) were kind gifts from Dr. John Cleveland (St. Jude Children's Research Hospital). Retroviral supernatants were prepared as described previously from HEK293T cells.[44] RD cells were incubated overnight with viral supernatant in the presence of polybrene (8 μg/ml; Sigma). After 24 h, the supernatant was discarded and RD cells incubated for a further 24 h with fresh viral supernatant. Viral-transduced RD cells were then incubated at 37°C in non-viral media for an additional 48 h. The viral-transduced cells were sorted by expression of GFP using fluorescence-activated cell sorting (MoFlo, Dako, Ft. Collins, CO, USA), and stable GFP-positive cells selected. RD-MDM2 cells or RD-neo cells were generated by stable transfection of pCMVneoMDM2 or pCMVneo-plasmids respectively. Cells expressing MDM2 or the parental plasmid were selected using G418 (500 μg/ml). The expression of Bcl-2 and MDM2 were confirmed by Western blot. The effect of transfection on RD cell growth was determined and plating density adjusted before treatment as for other RMS cell lines.

DNA cell cycle analysis. Cells were detached in phosphate-buffered saline (PBS)/2 mM EDTA, centrifuged at 1000 r.p.m. for 5 min, then gently resuspended in 250 μl hypotonic fluorochrome solution (PBS, 50 μg propidium iodide, 0.1% sodium citrate and 0.1% Triton X-100). The DNA content was analyzed by flow cytometry (Becton Dickinson FACScalibur; San Diego, CA, USA). Twenty thousand events were analyzed per sample and apoptosis was determined from the sub-G_0/G_1 DNA content.[3] The percentage of nuclei in the G_0/G_1 phase of the cell cycle was quantified using ModFit LT 3.1 (Verity Software House, Topsham, ME, USA) and the apoptotic fraction was excluded mathematically from the analysis.

M-phase analysis: immunofluorescent detection of phosphorylated-histone H3 (Ser10). Cells were harvested following C_6-ceramide/ASMase/nocodazole exposure and fixed in 70% ethanol overnight at −20°C. Cells were then washed twice with ice cold PBS, resuspended in 0.25% Triton X-100 in PBS and incubated at room temperature for 15 min. Cells were washed twice with PBS, resuspended in 100 μl 1% BSA in PBS containing 0.75 μg of anti-phospho-histone H3 (Ser10; Upstate Biotechnology, Lake placid, NY, USA) and incubated at room temperature for 3 h. Cells were pelleted, washed twice with PBS containing 1% BSA and then incubated for a further 30 min in the dark at room temperature with FITC-conjugated goat anti-rabbit IgG secondary antibody (Jackson ImmunoResearch Laboratories Inc., West Grove, PA, USA.) diluted at a ratio of 1 : 30 with PBS containing 1% BSA. Cells were washed and resuspended in PBS containing 1% BSA and 50 μg/ml propidium iodide. Samples were then analyzed for phosphorylated histone H3 and PI fluorescence by flow cytometry.

BrdU labeling and staining. Cells were pulse labeled with 10 μM 5-bromo-2′-deoxy-uridine (BrdU) for 30 min at 37°C under aseptic conditions. Cells were washed twice with media to remove free BrdU and then treated with C_6-ceramide/ASMase. Cells were harvested at various time points. BrdU incorporation and DNA content were determined using the 'APC BrdU Flow Kit' according to the manufacturers instructions (Becton Dickinson) by flow cytometry (Becton Dickinson FACScalibur**).**

Detection of double-strand breaks (DSB): immunofluorescent detection of phosphorylated-Histone H2A.X. (Ser139). Cells were treated with C_6-ceramide for 24 h and adherent cells washed in PBS and fixed for 10 min with PBS and 3% paraformaldehyde on ice. Cells were permeabilized for 30 min with PBS, 0.02% Triton X-100, washed three times with PBS, blocked 30 min with PBS, 3% BSA and then incubated with anti-phospho-histone H2A.X (Ser139, clone JBW01 Upstate Biotechnology, Lake placid, NY, USA) diluted 1 : 100 (v/v) at room temperature for 1 h with rotation. After three washes, cells were incubated with the Alexa Fluor™ 594-conjugated goat anti-mouse antibody (Molecular Probes, Eugene, USA) at 1 : 200 (v/v) dilution for 1 h at room temperature with rotation and subsequently washed three further times with PBS. Nuclei were stained with TO-PRO 3 (Molecular Probes) and sealed using mounting medium (Sigma, St. Louis, MO, USA). Images were obtained using a Leica TCS SP confocal microscope (Leica Microsystems Inc., Germany). The resulting data did not receive manipulation by computer imaging software.

Western blotting. After treatment, cells were detached in PBS/2 mM EDTA, centrifuged at 1,000 r.p.m. for 5 min, and lysed in 50 μl of ice-cold RIPA buffer supplemented with protease and phosphatase inhibitors. Protein concentrations were determined by the BioRad protein assay (BioRad, Hercules, CA, USA) according to the manufacturers' instructions; 50 μg of protein was electrophoresed by SDS-PAGE (BioRad, Hercules, CA, USA). Separated proteins were transferred to PVDF membranes (Millipore, Bedford, MA, USA). Blots were probed with anti-$p21^{Cip1/Waf1}$ (clone C19), $p27^{Kip1}$ (clone F-8) and MDM2 (clone N-20; all Santa Cruz Biotechnology, La Jolla, CA, USA), anti-PARP (C2-10), anti-Bcl-2 (clone 7; both BD Transduction Laboratories, San Diego, CA, USA), anti-Retinoblastoma (Rb; detects dephosphorylated and phosphorylated forms of Rb; clone G3-245; BD Pharmingen) or β-actin (Abcam, Cambridge, UK) followed by HRP-conjugated antibodies (KPL Inc., Gaithersburg, MD, USA). The ECL chemiluminescence system (Pierce Biotechnology Inc., Rockford, IL, USA) followed by exposure to CL-Xposure films (Kodak, Rochester, NY, USA) was used to visualize proteins.

RNA isolation and reverse transcription polymerase chain reaction (RT-PCR) analysis. RNA was isolated from RD cells using Trizol (Invitrogen Corporation, Carlsbad, CA, USA) and reverse transcribed using the Advantage® RT-for-PCR Kit (Clontech, Mountain View, CA, USA), according to the manufacturer's instructions. cDNA was amplified using standard PCR conditions. Briefly, amplifications were performed in 50 μl reactions comprising approximately 50 ng DNA, 10 × PCR buffer, 5 × Q-solution, 1.5 mM $MgCl_2$, 0.5 μM of each primer, 2.5 U Taq DNA polymerase (Qiagen, Valencia, CA, USA), 0.1 mM dNTPs and nuclease free water (Promega, Madison WI, USA). Primer sequences were as follows: 5′-TGTCAAACGTGCGAGTGTCTAACGG-3′ sense and 5′-AAGATCAGCCGGCGTTTGGA-3′ antisense for $p21^{Cip1/Waf1}$ (Accession number NM-/000389), 5′-TGTCAAACGTGCCAGTGTCTAACGG-3′ sense and 5′-TTTGACGTCTTCTGAGGCCAGGCTT-3′ antisense for $p27^{KIP1}$ (Accession number NM-/004064), 5′-ACGTGGTGGATCTGTGCAAAGAACC-3′ sense and 5′-TGCAGACTGATTGTCATGGTGGCTG-3′ antisense for p53 (Accession number NM-/000546), 5′-CAGCTCCTGTGCTGCGAAGTGGAA-3′ sense and 5′-CAGGCTTGACTCCAGCAGGGCTTC-3′ antisense for Cyclin D1 (Accession number 053056). Primers were designed using Vector NTI Advance 9 software (Invitrogen, Carlsbad, CA, USA). All primers were synthesized by the Hartwell Center (St. Jude Children's Research Hospital). PCR reactions were amplified using a MJ PTC-100™ Programmable Thermal Controller (Bio-Rad, Hercules, CA, USA) using the following cycling protocol, where *X* represents the annealing temperature: 94°C for 2 min, *X*°C for 45 s, 72°C for 2 min (first cycle), 94°C for 45 s and 72°C for 2 min for 30 cycles. The final cycle was modified to allow a 10 min extension at 72°C annealing temperatures were as follows: 54°C for $p21^{Cip1/Waf1}$ 58°C for $p27^{KIP1}$ 57°C for p53 and 59°C for Cyclin D1. In all, 40% of each PCR product was electrophoresed along with 500 ng of 100 bp ladder (Promega, Madison, WI, USA) on a 1% agarose gel at 100 V for 45 min to confirm product purity and correct size. Cycle sequencing reactions were performed using the ABI Prism Big Dye™ Terminator Sequencing kit version 3.0 (Applied Biosystems, Forest City, CA, USA) at the Hartwell Center (St. Jude Children's Research Hospital). Sequences were analyzed using the pairwise BLAST alignment method (National Center for Biotechnology Information, http://www.ncbi.nlm.nih.gov).

Small interfering RNA system and transfection. Small interfering RNAs were synthesized by Dharmacon Research Inc. (Lafayette, CO, USA). The siRNA consisted of a mixture of four siRNA duplexes targeting four different regions of the $p21^{Cip1/Waf1}$ mRNA (siGENOME SMARTpool p21, M-003308-00; $siRNA_{p21}$) or MDM2 mRNA (siGENOME SMARTpool MDM2, L-003279-00; $siRNA_{MDM2}$). A pool of four non-targeting siRNA duplexes was used as a negative control (siCONTROL non-targeting siRNA pool, D-001206-13; $siRNA_{ctrl}$). Transfection of cells with siRNA duplexes was performed using Lipofectamine 2000 (Invitrogen Corporation). To determine the optimum conditions for MDM2 or $p21^{Cip1/Waf1}$ downregulation, cells were transfected with 0, 25, 50 and 100 nM of $siRNA_{ctrl}$, $siRNA_{MDM2}$, $siRNA_{p21}$ for 0, 24, 48 or 72 h as recommended by Dharmacon. The downregulation of MDM2 or $p21^{Cip1/Waf1}$ was determined by Western blot or RT-PCR respectively. Subsequently, cells were transfected with 100 nM of $siRNA_{ctrl}$, $siRNA_{MDM2}$ or $siRNA_{p21}$ for 48 h and following a change of media, treated for a further 24 h with the aforementioned agents.

Quantification of endogenous ceramide content. RD cells were treated with exogenous human ASMase for the indicated times, lipids were extracted and the endogenous levels of ceramide were determined by the diacylglycerol kinase (DAGK) assay as described elsewhere.[3]

Statistical analysis. Data are represented as the mean $\pm$ S.E.M. In all cases, n refers to the number of independent experiments. Statistical analyses were performed by the Student's *t*-test and analysis of variance (ANOVA), where $P<0.05$ was considered significant.

Acknowledgements. This study was supported by NCI awards CA 87952[1], CA 92401[2], the Cancer Center Core Grant CA 21765[2] and by the American Lebanese Syrian Associated Charities (ALSAC). We thank Dr. Michael Rainey (St. Jude Children's Research Hospital) for his critical review of this manuscript.

1. Ogretmen B, Hannun YA. Biologically active sphingolipids in cancer pathogenesis and treatment. *Nat Rev Cancer* 2004; **4**: 604–616.
2. Goni FM, Alonso A. Biophysics of sphingolipids I. Membrane properties of sphingosine. Ceramides and other simple sphingolipids. *Biochim Biophys Acta* 2006; **1758**: 1902–1921.
3. Phillips DC, Griffiths HR. Ceramide induces a loss in cytosolic peroxide levels in mononuclear cells. *Biochem J* 2003; **375**: 567–579.
4. Lee JY, Bielawska AE, Obeid LM. Regulation of cyclin-dependent kinase 2 activity by ceramide. *Exp Cell Res* 2000; **261**: 303–311.
5. Altura BM, Gebrewold A, Zheng T, Altura BT. Sphingomyelinase and ceramide analogs induce vasoconstriction and leukocyte-endothelial interactions in cerebral venules in the intact rat brain: insight into mechanisms and possible relation to brain injury and stroke. *Brain Res Bull* 2002; **58**: 271–278.
6. Martin S, Phillips DC, Szekely-Szucs K, Elghazi L, Desmots F, Houghton JA. Cyclooxygenase-2 inhibition sensitizes human colon carcinoma cells to TRAIL-induced apoptosis through clustering of DR5 and concentrating death-inducing signaling complex components into ceramide-enriched caveolae. *Cancer Res* 2005; **65**: 11447–11458.
7. Daido S, Kanzawa T, Yamamoto A, Takeuchi H, Kondo Y, Kondo S. Pivotal role of the cell death factor BNIP3 in ceramide-induced autophagic cell death in malignant glioma cells. *Cancer Res* 2004; **64**: 4286–4293.
8. Phillips DC, Allen K, Griffiths HR. Synthetic ceramides induce growth arrest or apoptosis by altering cellular redox status. *Arch Biochem Biophys* 2002; **407**: 15–24.
9. Lee JY, Leonhardt LG, Obeid LM. Cell-cycle-dependent changes in ceramide levels preceding retinoblastoma protein dephosphorylation in G2/M. *Biochem J* 1998; **334** (Part 2): 457–461.
10. Sherr CJ, Roberts JM. Inhibitors of mammalian G1 cyclin-dependent kinases. *Genes Dev* 1995; **9**: 1149–1163.
11. Bunz F, Dutriaux A, Lengauer C, Waldman T, Zhou S, Brown JP *et al.* Requirement for p53 and p21 to sustain G2 arrest after DNA damage. *Science* 1998; **282**: 1497–1501.
12. Jin Y, Lee H, Zeng SX, Dai MS, Lu H. MDM2 promotes p21waf1/cip1 proteasomal turnover independently of ubiquitylation. *EMBO J* 2003; **22**: 6365–6377.
13. Liu CW, Corboy MJ, DeMartino GN, Thomas PJ. Endoproteolytic activity of the proteasome. *Science* 2003; **299**: 408–411.
14. Sheaff RJ, Singer JD, Swanger J, Smitherman M, Roberts JM, Clurman BE. Proteasomal turnover of p21Cip1 does not require p21Cip1 ubiquitination. *Mol Cell* 2000; **5**: 403–410.
15. Zhang Z, Wang H, Li M, Agrawal S, Chen X, Zhang R. MDM2 is a negative regulator of p21WAF1/CIP1, independent of p53. *J Biol Chem* 2004; **279**: 16000–16006.
16. Corvi R, Savelyeva L, Breit S, Wenzel A, Handgretinger R, Barak J *et al.* Non-syntenic amplification of MDM2 and MYCN in human neuroblastoma. *Oncogene* 1995; **10**: 1081–1086.
17. Leach FS, Tokino T, Meltzer P, Burrell M, Oliner JD, Smith S *et al.* p53 Mutation and MDM2 amplification in human soft tissue sarcomas. *Cancer Res* 1993; **53**: 2231–2234.
18. Oliner JD, Kinzler KW, Meltzer PS, George DL, Vogelstein B. Amplification of a gene encoding a p53-associated protein in human sarcomas. *Nature* 1992; **358**: 80–83.
19. Reifenberger G, Liu L, Ichimura K, Schmidt EE, Collins VP. Amplification and overexpression of the MDM2 gene in a subset of human malignant gliomas without p53 mutations. *Cancer Res* 1993; **53**: 2736–2739.
20. Bartel F, Taylor AC, Taubert H, Harris LC. Novel mdm2 splice variants identified in pediatric rhabdomyosarcoma tumors and cell lines. *Oncol Res* 2000; **12**: 451–457.
21. Taylor AC, Shu L, Danks MK, Poquette CA, Shetty S, Thayer MJ *et al.* P53 mutation and MDM2 amplification frequency in pediatric rhabdomyosarcoma tumors and cell lines. *Med Pediatr Oncol* 2000; **35**: 96–103.
22. Zhang R, Wang H. MDM2 oncogene as a novel target for human cancer therapy. *Curr Pharm Des* 2000; **6**: 393–416.
23. Haupt Y, Maya R, Kazaz A, Oren M. Mdm2 promotes the rapid degradation of p53. *Nature* 1997; **387**: 296–299.
24. Pomerantz J, Schreiber-Agus N, Liegeois NJ, Silverman A, Alland L, Chin L *et al.* The Ink4a tumor suppressor gene product, p19Arf, interacts with MDM2 and neutralizes MDM2's inhibition of p53. *Cell* 1998; **92**: 713–723.
25. Martin K, Trouche D, Hagemeier C, Sorensen TS, La Thangue NB, Kouzarides T. Stimulation of E2F1/DP1 transcriptional activity by MDM2 oncoprotein. *Nature* 1995; **375**: 691–694.
26. Balint E, Bates S, Vousden KH. Mdm2 binds p73 alpha without targeting degradation. *Oncogene* 1999; **18**: 3923–3929.
27. Breitfeld PP, Meyer WH. Rhabdomyosarcoma: new windows of opportunity. *Oncologist* 2005; **10**: 518–527.
28. Gartel AL, Tyner AL. The role of the cyclin-dependent kinase inhibitor p21 in apoptosis. *Mol Cancer Ther* 2002; **1**: 639–649.
29. Garcia-Ruiz C, Mari M, Morales A, Colell A, Ardite E, Fernandez-Checa JC. Human placenta sphingomyelinase, an exogenous acidic pH-optimum sphingomyelinase, induces oxidative stress, glutathione depletion, and apoptosis in rat hepatocytes. *Hepatology* 2000; **32**: 56–65.
30. Reed JC. Bcl-2 family proteins: regulators of apoptosis and chemoresistance in hematologic malignancies. *Semin Hematol* 1997; **34**: 9–19.
31. Kang KH, Kim WH, Choi KH. p21 promotes ceramide-induced apoptosis and antagonizes the antideath effect of Bcl-2 in human hepatocarcinoma cells. *Exp Cell Res* 1999; **253**: 403–412.
32. Oh WJ, Kim WH, Kang KH, Kim TY, Kim MY, Choi KH. Induction of p21 during ceramide-mediated apoptosis in human hepatocarcinoma cells. *Cancer Lett* 1998; **129**: 215–222.
33. Alesse E, Zazzeroni F, Angelucci A, Giannini G, Di Marcotullio L, Gulino A. The growth arrest and downregulation of c-myc transcription induced by ceramide are related events dependent on p21 induction, Rb underphosphorylation and E2F sequestering. *Cell Death Differ* 1998; **5**: 381–389.
34. Taylor WR, Stark GR. Regulation of the G2/M transition by p53. *Oncogene* 2001; **20**: 1803–1815.
35. Dash BC, El-Deiry WS. Phosphorylation of p21 in G2/M promotes cyclin B-Cdc2 kinase activity. *Mol Cell Biol* 2005; **25**: 3364–3387.
36. Dbaibo GS, Pushkareva MY, Jayadev S, Schwarz JK, Horowitz JM, Obeid LM *et al.* Retinoblastoma gene product as a downstream target for a ceramide-dependent pathway of growth arrest. *Proc Natl Acad Sci USA* 1995; **92**: 1347–1351.
37. Spyridopoulos I, Mayer P, Shook KS, Axel DI, Viebahn R, Karsch KR. Loss of cyclin A and G1-cell cycle arrest are a prerequisite of ceramide-induced toxicity in human arterial endothelial cells. *Cardiovasc Res* 2001; **50**: 97–107.
38. Zhu XF, Liu ZC, Xie BF, Feng GK, Zeng YX. Ceramide induces cell cycle arrest and upregulates p27kip in nasopharyngeal carcinoma cells. *Cancer Lett* 2003; **193**: 149–154.
39. Rani CS, Abe A, Chang Y, Rosenzweig N, Saltiel AR, Radin NS *et al.* Cell cycle arrest induced by an inhibitor of glucosylceramide synthase. Correlation with cyclin-dependent kinases. *J Biol Chem* 1995; **270**: 2859–2867.
40. Zhou BB, Chaturvedi P, Spring K, Scott SP, Johanson RA, Mishra R *et al.* Caffeine abolishes the mammalian G(2)/M DNA damage checkpoint by inhibiting ataxia-telangiectasia-mutated kinase activity. *J Biol Chem* 2000; **275**: 10342–10348.
41. Skapek SX, Rhee J, Spicer DB, Lassar AB. Inhibition of myogenic differentiation in proliferating myoblasts by cyclin D1-dependent kinase. *Science* 1995; **267**: 1022–1024.
42. Gartel AL, Radhakrishnan SK. Lost in transcription: p21 repression, mechanisms, and consequences. *Cancer Res* 2005; **65**: 3980–3985.
43. Hazelton BJ, Houghton JA, Parham DM, Douglass EC, Torrance PM, Holt H *et al.* Characterization of cell lines derived from xenografts of childhood rhabdomyosarcoma. *Cancer Res* 1987; **47**: 4501–4507.
44. Phillips DC, Martin S, Doyle BT, Houghton JA. Sphingosine-induced apoptosis in rhabdomyosarcoma cell lines is dependent on pre-mitochondrial Bax activation and post-mitochondrial caspases. *Cancer Res* 2007; **67**: 756–764.

Supplementary Information accompanies the paper on Cell Death and Differentiation website (http://www.nature.com/cdd)